Biochemical and Biophysical Research Communications 484 (2017) 365–371

Contents lists available at ScienceDirect

Biochemical and Biophysical Research Communications

journal homepage: www.elsevier.com/locate/ybbrc

7-(4-Hydroxy-3-methoxyphenyl)-1-phenyl-4*E*-hepten-3-one alleviates Aβ_{1-42} induced cytotoxicity through PI3K-mTOR pathways

Hanlin Xiao, Qinghua Zhang, Yinghui Peng, Genyun Tang, Yumei Liao, Xiaoji Zhuang, Wen-Cai Ye, Ying Wang, Lei Shi*

JNU-HKUST Joint Laboratory for Neuroscience and Innovative Drug Research, Jinan University, Guangzhou, 510632, Guangdong, China

ARTICLE INFO

Article history:
Received 13 January 2017
Accepted 23 January 2017
Available online 25 January 2017

Keywords:
Alzheimer's disease
Diarylheptanoid
Reactive oxygen species
Caspase-3
Dendrite
Neuroprotection

ABSTRACT

Alzheimer's disease (AD) is the most common neurodegenerative disease in the elderly. Increasing evidence has shown that β-amyloid protein (Aβ) production is the key pathological cause of AD. 7-(4-Hydroxy-3-methoxyphenyl)-1-phenyl-4*E*-hepten-3-one (AO-2), a natural diarylheptanoid, is previously found to have activities in neuronal differentiation and neurite outgrowth, and its analogue shows protective effects against Aβ. In this study, we further investigated the function of AO-2 toward Aβ-induced injuries in PC12 cells and hippocampal neurons. Pretreatment of PC12 cells with AO-2 restored cell viability in a concentration-dependent manner against Aβ-induced neurotoxicity. Moreover, the Aβ stimulated apoptosis and caspase-3 activation were markedly inhibited by AO-2. We found that AO-2 prevented the downregulation of PI3K-Akt-mTOR signaling after Aβ damage, and blockade of either PI3K or mTOR activity led to the failure of AO-2 on caspase-3 inhibition. We further showed that AO-2 was protective against two devastating effects of Aβ, increased reactive oxygen species (ROS) production and dendrite injury, and this protection was also dependent on PI3K and mTOR activities. Taken together, this study showed that AO-2 acts against Aβ-induced damages in PC12 cells and hippocampal neurons through PI3K-mTOR pathways, thus providing a new neuroprotective compound which may shed light on drug development of AD.

1. Introduction

Alzheimer's disease (AD), the most common cause of dementia [1,2], is characterized by amyloid β (Aβ) deposits and neurofibrillary tangles [3–5]. Aβ_{1-42}, which consists of 42 amino acids of the peptide, is the most found toxic forms in the pathogenesis of AD [6,7]. Aβ_{1-42} causes oxidative stress which leads to DNA damage and caspase-dependent neuronal apoptosis, and this process plays an important role in neurodegeneration [8,9]. Moreover, there is cumulative evidence that dystrophic neurites and dendritic simplification are associated with AD [10,11]. Therefore, treatments that alleviate Aβ_{1-42} induced caspase-dependent apoptosis and impairments in dendrites may be a therapeutic approach for AD [12,13].

An increasing number of natural products have been served as the source for drug development of AD, such as curcumin and resveratrol [14,15]. Our previous study showed that 7-(4-hydroxyphenyl)-1-phenyl-4*E*-hepten-3-one (AO-1) and 7-(4-hydroxy-3-methoxyphenyl)-1-phenyl-4*E*-hepten-3-one (AO-2; Fig. 1A), two closely related, curcumin-like diarylheptanoids, promote differentiation and neurite outgrowth of neuroblastoma cells and hippocampal neurons [16]. AO-1 also shows a neuroprotective effect against Aβ_{1-42} induced toxicity [17]. However, whether AO-2 is another beneficial compound against Aβ_{1-42} is still unknown.

In the present study, we first examined the protective effects of AO-2 in PC12 cells, a well-established neuronal cell line for neuroprotective studies. Cytotoxicity, apoptosis, and the reactive oxygen species (ROS) levels were measured to evaluate the effects of AO-2 in the presence of Aβ_{1-42}. Moreover, we used primary hippocampal neurons to study whether neuronal death and dendritic injury induced by Aβ_{1-42} were attenuated or rescued by AO-2. We also explored the molecular action of AO-2 by examining cleaved caspase-3 production and several signaling pathways. Our study demonstrated that AO-2 exhibited potent neuroprotective effects against neuronal apoptosis, ROS production, and dendritic damages induced by Aβ_{1-42}, which was dependent on PI3K-mTOR pathway.

* Corresponding author. JNU-HKUST Joint Laboratory for Neuroscience and Innovative Drug Research, 2nd Building of Sci. & Tech., Jinan University, Guangzhou, 510632, China.
E-mail address: sophielshi80@gmail.com (L. Shi).

http://dx.doi.org/10.1016/j.bbrc.2017.01.125
0006-291X/

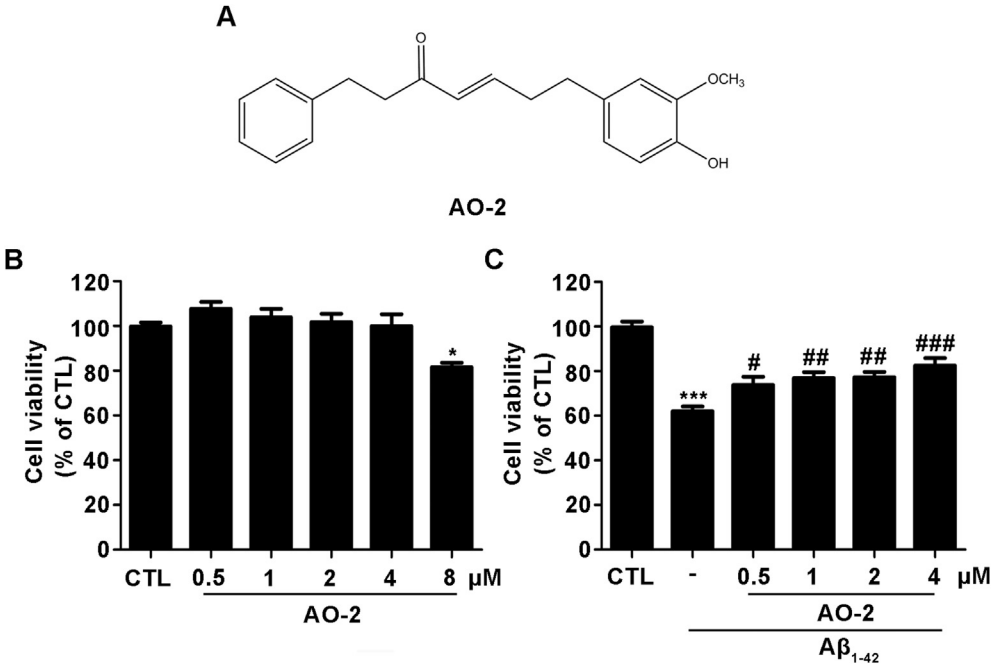

Fig. 1. Protective effects of AO-2 against $A\beta_{1-42}$-induced cytotoxicity in PC12 cells. A. The chemical structure of AO-2 is shown. B. PC12 cells were exposed to indicated concentrations of AO-2 and cell viability was determined at 24 h later by MTT assay. $^{*}P < 0.05$, AO-2 (8 μM) vs. CTL (control). C. AO-2 prevents $A\beta_{1-42}$ induced decrease of cell viability. PC12 cells were pretreated with different concentrations of AO-2 (0.5, 1, 2, 4 μM) for 2 h followed by exposure to 1 μM $A\beta_{1-42}$ for 24 h. Cell viability was determined using MTT assay. $^{***}P < 0.001$, $A\beta_{1-42}$ vs. CTL. $\#P < 0.05$, $\#\#P < 0.01$ and $\#\#\#P < 0.001$, AO-2 + $A\beta_{1-42}$ vs. $A\beta_{1-42}$ alone. For B and C, Data are expressed as percentages of values of that in untreated control cells, and are expressed as mean ± SEM of three independent experiments.

2. Materials and methods

2.1. Chemicals, reagents and materials

AO-2 (7-(4-hydroxy-3-methoxyphenyl)-1-phenyl-4*E*-hepten-3-one) was extracted from the rhizomes of *A. officinarum* Hance as previously reported [16]. Stock AO-2 was dissolved in DMSO at a concentration of 10 mM. Different concentrations of AO-2 (0.5–8 μM) was used to study its protective effects, and DMSO with the volume equal to the highest concentration of AO-2 was added as the vehicle control in each experiment.

Rabbit monoclonal antibodies against caspase-3, p38, Akt and S6K were purchased from Cell Signaling Technology; α-tubulin was from Sigma-Aldrich; GAPDH was from Abcam; Anti-Microtubule-Associated Protein 2 (MAP2) antibody and LY294002 were from Millipore; Torin1 was from Tocris; 2′, 3-(4,5-dimethylthiazol-2-yl)-2,5-diphenyl tetrazolium bromide (MTT), dimethyl-sulfoxide (DMSO) and curcumin were from Sigma-Aldrich.

2.2. Preparation of oligomerized $A\beta_{1-42}$

$A\beta_{1-42}$ was purchased from rPeptide and was dissolved in phosphate-buffered saline (PBS) at a concentration of 1 mM. Prior to the treatment, peptides were preincubated at 37 °C for 7 days to promote aggregation and then diluted in medium to desired concentrations as described previously [17]. Soluble oligomerized $A\beta_{1-42}$ peptides (equivalent to 1 μM peptides) were added to cells to induce damaging effects.

2.3. Cell culture

PC12 cells were obtained from the American Type Culture Collection (ATCC) and were cultured in Dulbecco's modified Eagle's medium supplemented with 6% FBS, 6% HS and 1% penicillin/streptomycin under a humidified atmosphere of 5% CO_2 and 95% air at 37 °C. Cells were plated at 1×10^4 cells per well in 96 well plates for cytotoxicity study, 3×10^5/35 mm dish for flow cytometry and western blot analysis.

Primary hippocampal neurons were prepared from E18 Sprague Dawley (SD) rat embryos as previously described [18]. Briefly, Rat hippocampal neurons (1×10^5 per coverslip) were plated on 18 mm coverslips coated with poly-D-lysine (1 mg/ml; Sigma) and fed with 0.2% B27 (Invitrogen), 1 mM L-glutamine (Life Technologies) and 1% penicillin/streptomycin. All experimental procedures involving the use of animals were approved by the Ethics Committee on Animal Experiments at Jinan University, China, and were strictly performed according to the guidelines of the Care and Use of Laboratory Animals.

2.4. Measurement of cell viability

PC12 cells were preincubated with AO-2 for 2 h and exposed to 1 μM $A\beta_{1-42}$ for 24 h, and cell viability was measured by MTT assay as previously reported [16]. Briefly, MTT was added to each well for 4 h, and then the formazan was dissolved in DMSO. The optical density (OD) values were detected at 595 nm in a multimode detector (Beckman coulter). Cell viability was expressed as a percentage of the value against the control using the following formula: Cell viability (%) = (absorption of sample - absorption of background)/(absorption of control - absorption of background) × 100%.

2.5. Detection of apoptosis by flow cytometry

The protective effect of AO-2 against cell apoptosis was evaluated using the Annexin V-fluorescein isothiocyanate (FITC)/propidium iodide (PI) Apoptosis Detection Kit (Biouniquer Tech) according to the manufacturer's instructions. Briefly, cells were

harvested by centrifugation, washed twice with cold PBS and resuspended in 1 × Annexin-binding buffer at a concentration of 1×10^6 cells/ml. After transferring to a 5 ml culture tube, Annexin V-FITC and PI were added, and the cells were gently vortexed and incubated at room temperature in the dark. Finally, 1 × Annexin-binding buffer was added to each tube, and the samples were mixed gently and kept on ice. The apoptosis rate was analyzed by flow cytometry (Millipore) within 1 h.

2.6. TUNEL/DAPI double staining assay

Hippocampal neurons were plated at the density of 1×10^5/coverslip. As previously described, a TUNEL/DAPI staining kit (Roche) was used to determine cell apoptosis [16]. Briefly, cells were fixed with 4% paraformaldehyde (Sigma-Aldrich), washed with PBS, permeabilized with 0.1% sodium citrate and 0.1% Triton X-100 for 2 min, followed by treatment with TUNEL reaction mixture. The cells were imaged with Zeiss Axio Imager A2 microscope (Carl Zeiss AG) and the numbers of TUNEL-positive (apoptotic) cells were counted. The apoptosis rate (%) was counted by ImageJ software (National Institutes of Health, Bethesda, Maryland, USA).

2.7. Western blotting analysis

Cells were washed with ice-cold PBS and were lysed in RIPA buffer for 30 min on ice. Protein concentration was quantified using the BCA assay kit. Samples were subjected to SDS-PAGE on 12% gel and were transferred to PVDF membranes. The membranes were probed with the indicated antibodies, followed by secondary antibodies (Anti-Mouse and Anti-Rabbit antibodies, Cell Signaling), Detection was performed using ECL Plus (GE Healthcare). The density of bands was measured using Quantity One analysis software.

2.8. Determination of intracellular ROS levels

The relative levels of ROS were examined as previously reported [17]. Briefly, PC12 cells were seeded in 96-well plates at a density of 1×10^4 cells/well and incubated for 24 h. AO-2 was added for 2 h, then co-incubated with 1 μM $A\beta_{1\text{-}42}$ for 24 h. One hour prior to AO-2 treatment, PI3K inhibitor (LY294002, 10 μM) and mTOR inhibitor (Torin1, 50 nM) were added to cells. Afterwards, 2′, 7′-dichlorofluorescin diacetate (DCFH-DA; 5 μM; Life Technologies) was added and incubated for 30 min in the dark, followed by washing with DPBS. The ROS levels were determined at excitation and emission wavelengths of 488 nm and 528 nm, respectively, by a DTX880 multimode detector (Beckman Coulter, Brea, CA, USA).

2.9. Morphological analysis of dendrites

Hippocampal neurons were exposed to AO-2 for 2 h, followed by co-treatment of AO-2 and $A\beta_{1\text{-}42}$ for 24 h. Neurons were stained with the dendrite marker MAP2. For inhibitor treatment assay, hippocampal neurons were pretreated with 10 μM LY294002 and 50 nM Torin1 for 60 min, followed by AO-2 treatment for 2 h. $A\beta_{1\text{-}42}$ was then added to the hippocampal neurons for 24 h. Dendrites were visualized by immunostaining with MAP2. The number of positive cells was counted from photographs obtained by Zeiss 700 confocal microscope (Carl Zeiss AG). Ten fields per coverslip in three separated experiments were selected. Total dendritic branch points were counted by using ImageJ software.

2.10. Statistical analysis

All statistical analyses were performed using Graphpad Prism 5 and all data were expressed as mean ± standard error of the mean (SEM). Each experiment was repeated at least three times. One-way ANOVA followed by Bonferroni's Multiple Comparison Test was used.

3. Results

3.1. $A\beta_{1-42}$-induced cytotoxicity was attenuated by AO-2

To test the nontoxic dosage of AO-2 treatment, the effects of AO-2 at a range of concentrations (0.5–8 μM) on cell viability of PC12 cells were measured, and the results showed that AO-2 at 0.5–4 μM had no obvious cytotoxicity after treatment for 24 h (Fig. 1B). These concentrations were consistent with those used for neurite outgrowth in neuroblastoma cells and hippocampal neurons [16]. To examine whether AO-2 could protect PC12 cells from $A\beta_{1-42}$ toxicity, cells were preincubated with 0.5–4 μM AO-2 for 2 h and exposed to 1 μM $A\beta_{1-42}$ for 24 h. The viability of PC12 cells decreased to only ~60% of the control group after 24 h treatment with 1 μM $A\beta_{1-42}$ (Fig. 1C). However, cells pretreated with AO-2 had increasingly restored viability along with the increase of AO-2 concentration, i.e., 73.42% ± 3.91%, 76.55% ± 2.90%, 76.92% ± 2.69% and 81.76% ± 3.35% viability comparing to the control group when the concentration of AO-2 was 0.5, 1, 2, 4 μM, respectively (Fig. 1C). Therefore, AO-2 pretreatment significantly ameliorated $A\beta_{1\text{-}42}$-induced toxicity in a dose-dependent manner.

3.2. AO-2 protects against $A\beta_{1\text{-}42}$-induced apoptosis

$A\beta_{1\text{-}42}$ induced cell injury eventually leads to neuronal death. We used Annexin V/propidium iodide (PI) double labeling method followed by flow cytometry to determine apoptotic and necrotic cells. Apoptotic cells are labeled by Annexin V, which binds to the apoptotic marker phosphatidylserine at outer leaflet of the plasma membrane; whereas necrotic or dead cells are labeled by PI, which binds to nuclei acid and is impermeable to viable cells (Fig. 2A). The results showed that 4 μM AO-2 pretreatment totally blocked cell apoptosis and necrosis induced by $A\beta_{1\text{-}42}$ in PC12 cells (Fig. 2B and C). This anti-apoptotic effect of AO-2 was equivalent to curcumin (10 μM), a well know neuroprotective compound that is structurally similar to AO-2 [21].

To test whether AO-2 acts against the apoptotic effect of $A\beta_{1\text{-}42}$ in hippocampal neurons, we evaluated DNA damage-induced apoptosis using TUNEL staining. $A\beta_{1\text{-}42}$ treatment led to more apoptosis as indicated by increased TUNEL labeling (26.34% comparing to 15.54% in control). Similar as what was observed in PC12 cells, pretreatment of AO-2 (4 μM) exhibited neuroprotective effects which restored normal apoptotic rate in hippocampal neurons (Fig. 2D and E).

3.3. AO-2 inhibits $A\beta_{1\text{-}42}$ induced caspase-3 activation through PI3K-Akt-mTOR pathway

Activation of caspase pathway is a critical event during apoptosis. Hence, we measured the expression of the cleaved caspase-3, which indicates the level of caspase activation. $A\beta_{1\text{-}42}$ triggered elevated cleavage of caspase-3, whereas 4 μM AO-2 or 10 μM curcumin pretreatment totally reversed the upregulated cleaved caspase-3 back to normal levels (Fig. 3A and B).

Activation of the mitogen-activated protein kinase (MAPK) p38 is closed related to apoptosis and caspase activation. P38 is also a master kinase that triggers neuroinflammatory responses [19]. We found that $A\beta_{1\text{-}42}$ induced p38 phosphorylation was totally inhibited by AO-2 (Fig. 3A and C). Interestingly, the effect of 1 μM AO-2 was comparable to 10 μM curcumin, and 2 or 4 μM AO-2 even

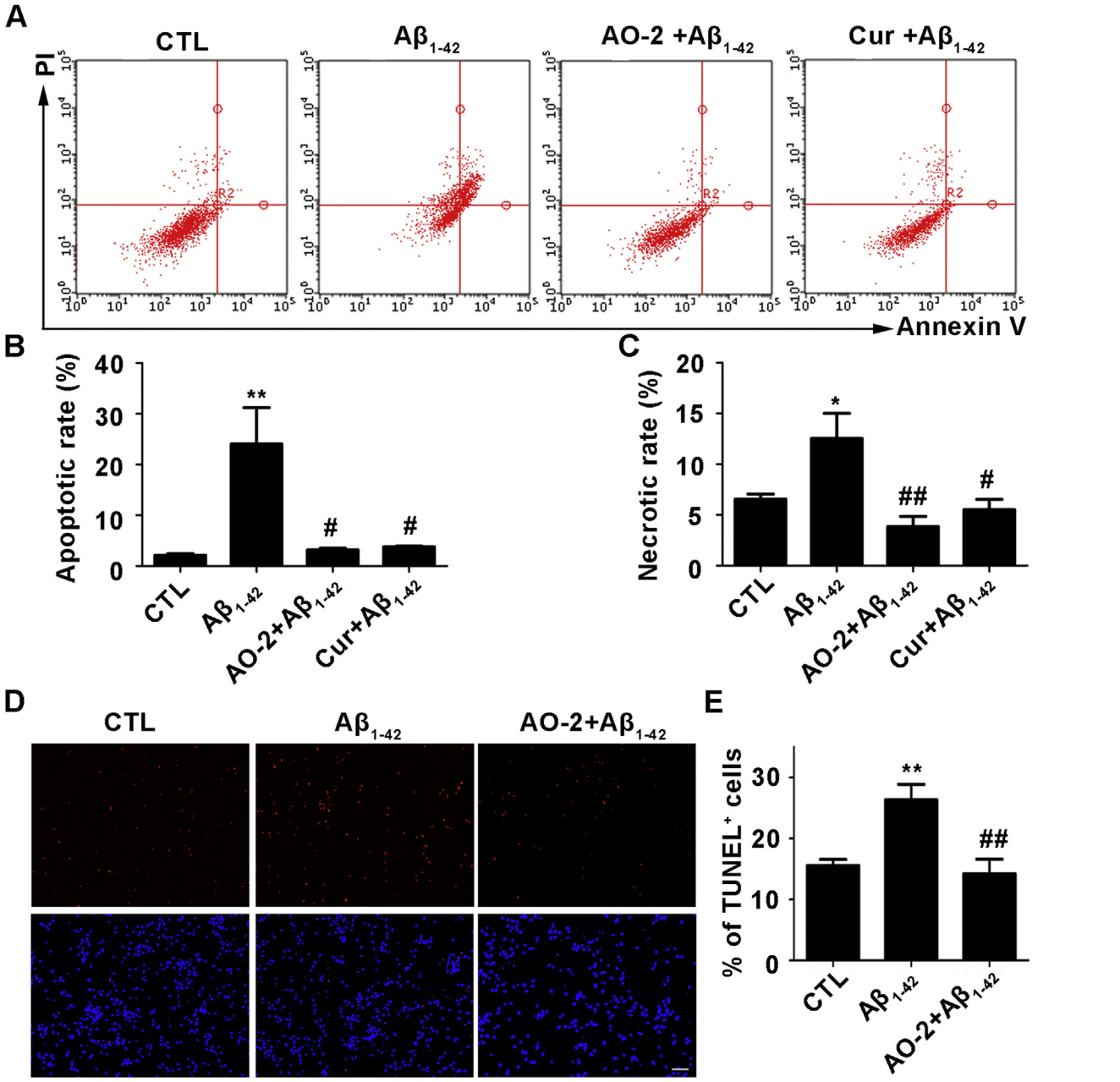

Fig. 2. AO-2 prevented $A\beta_{1-42}$ induced apoptosis. **A**. PC12 cells were pretreated with DMSO, 4 μM AO-2 or 10 μM Cur for 2 h followed by 1 μM $A\beta_{1-42}$ for 24 h. Quantification of apoptotic cells (AV^+/PI^- and AV^+/PI^+; **B**) and necrotic cells (AV^-/PI^+; **C**). **D, E**. Apoptotic cell death was measured using TUNEL/DAPI double staining kit. Scale bar, 50 μm. Data are expressed as mean ± SEM of three independent experiments. $^*P < 0.05$ and $^{**}P < 0.01$, $A\beta_{1-42}$ vs. CTL; $\#P < 0.05$, $\#\#P < 0.001$, AO-2 + $A\beta_{1-42}$ or Cur + $A\beta_{1-42}$ vs. $A\beta_{1-42}$ alone.

further reduced p38 phosphorylation. These results suggest that AO-2 may have both anti-apoptosis and anti-inflammatory effects.

As PI3K-mTOR pathway has been shown important in mediating neuroprotective effects of AO-1 [17], we asked whether this signaling pathway also contributes to AO-2's effect. Indeed, $A\beta_{1-42}$ led to marked downregulation of both Akt and pS6K, a downstream kinase of PI3K-Akt-mTOR pathway, whereas AO-2 prevented the decrease of Akt and pS6K activities (Fig. 3D, G and H). Importantly, addition of either PI3K inhibitor LY294002 or mTOR inhibitor Torin 1 totally blocked the effects of AO-2 on the inhibition of cleaved caspase-3 (Fig. 3E, F, I and J). Thus, PI3K-mTOR pathway is important for the neuroprotection effects of AO-2 against $A\beta_{1-42}$ induced caspase-3 cleavage.

3.4. AO-2 prevents $A\beta_{1-42}$-induced ROS production and dendritic abnormalities through PI3K-mTOR pathway

Oxidative stress caused by augmented accumulation of intracellular ROS is one of the main causes of neuronal death in AD [20]. To investigate whether AO-2 has an antioxidant activity against Aβ, we evaluated ROS production after AO-2 was co-treated with $A\beta_{1-42}$. The accumulation of ROS was detected by DCFH-DA assay, which measures intracellular ROS by the conversion of DCFH-DA into the fluorescent probe DCF. After exposure to $A\beta_{1-42}$, ROS levels increased ~50% comparing to control (Fig. 4A). In contrast, treatment of AO-2 at 0.5–4 μM or curcumin at 10 μM totally restored ROS production to normal levels, suggesting that AO-2 has strong antioxidant effect against $A\beta_{1-42}$. Importantly, the ROS inhibition by

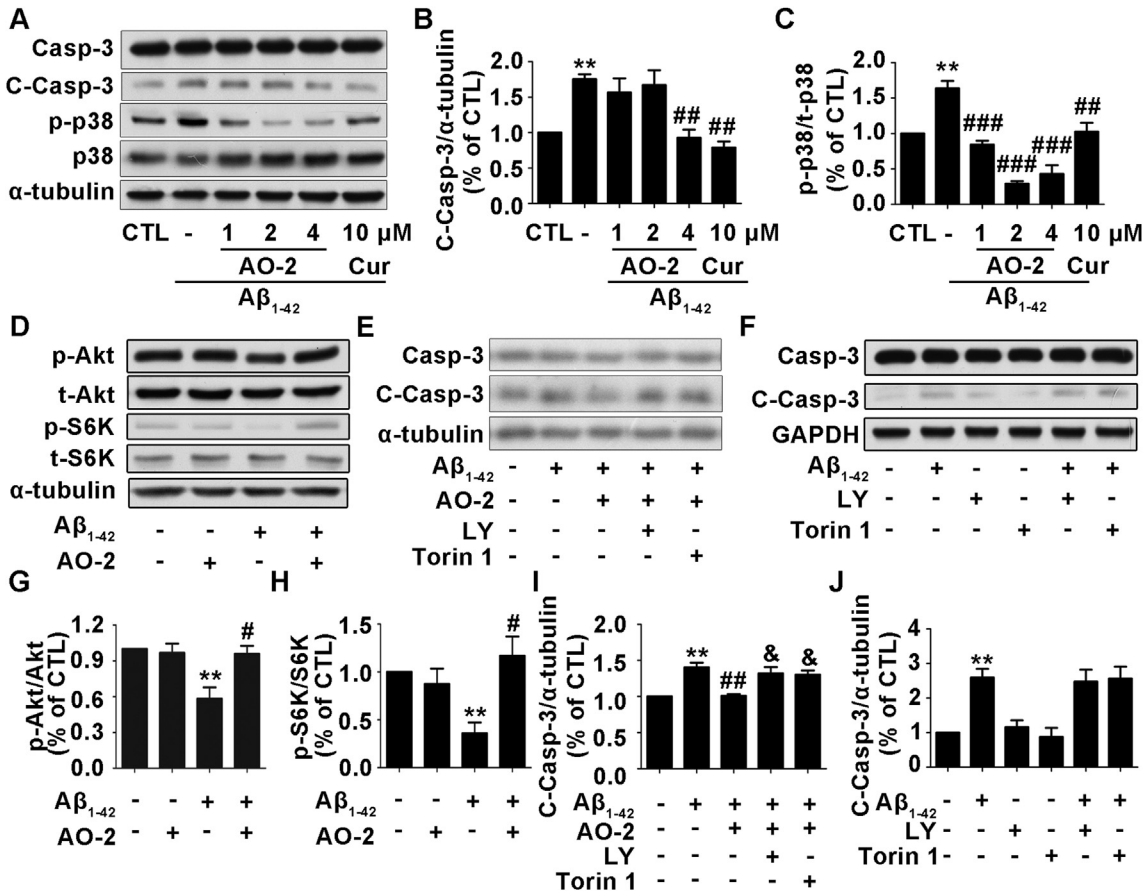

Fig. 3. AO-2 inhibits cleaved caspase-3 (C-Casp-3) and phosphorylation of p38 induced by $A\beta_{1\text{-}42}$. Cells were pretreated with LY294002 (LY) or Torin-1 for 1 h and then exposed to AO-2 for 2 h, followed by 1 μM $A\beta_{1\text{-}42}$ for 24 h. **A**. Caspase-3 (Casp-3), C-Casp-3, p38 and phosphorylated p38 (p-p38) levels were detected by western blotting. **B, C**. Data are presented as C-Casp-3 or p-p38 band densities normalized to α-tubulin or GAPDH. **D**. AO-2 reversed $A\beta_{1\text{-}42}$-induced downregulation of Akt and pS6K. Total and phosphorylated proteins were all detected by western blotting. **E, F**. PC12 cells were stimulated with $A\beta_{1\text{-}42}$ (1 μM) in the presence of DMSO or AO-2 (4 μM) with LY294002 (LY), Torin-1 or DMSO prior to AO-2. After 24 h, the levels of C-Casp-3 were measured by western blot analysis. (**B, I** and **J**) Data are presented as C-Casp-3 band densities normalized to α-tubulin. (**C, G** and **H**) Data are presented as p-p38/p-Akt/p-pS6K band densities normalized to p38/Akt/pS6K, respectively. For **B, C, I** and **J**, $^{**}P < 0.01$, $A\beta_{1\text{-}42}$ vs. control; $^{\#\#}P < 0.01$, $^{\#\#\#}P < 0.001$, $A\beta_{1\text{-}42}$ + AO-2 or Cur vs. $A\beta_{1\text{-}42}$ alone; $^{\&}P < 0.05$, $A\beta_{1\text{-}42}$+AO-2+inhibtor vs $A\beta_{1\text{-}42}$+AO-2. For **G** and **H**, $^{**}P < 0.01$, $A\beta_{1\text{-}42}$ vs. control; $^{\#}P < 0.05$, $A\beta_{1\text{-}42}$ + AO-2 vs. $A\beta_{1\text{-}42}$ alone. Results were obtained from three separate experiments. Data are shown as mean ± SEM.

AO-2 was via activation of PI3K-mTOR pathway, as either LY294002 or Torin 1 blocked AO-2's effect (Fig. 4B).

During early pathogenesis of AD, $A\beta_{1\text{-}42}$ is believed to cause dendritic and synaptic impairments in hippocampal neurons [22]. So we detected the protective effect of AO-2 on $A\beta_{1\text{-}42}$-induced dendrite injury. $A\beta_{1\text{-}42}$ treatment in hippocampal neurons (7 DIV) for 24 h induced a marked atrophy of dendrites, indicated by the decrease of dendritic branches (Fig. 4C). When AO-2 was pretreated for 2 h, followed by co-treatment of AO-2 and $A\beta_{1\text{-}42}$ for 24 h, the dendrite morphology was substantially restored (Fig. 4C). Consistent with previous findings, addition of LY294002 and Torin1 totally blocked the effect of AO-2 on dendrite protection. These results together suggest that PI3K-Akt-mTOR pathway essentially contributes to AO-2 mediated protective effects against $A\beta_{1\text{-}42}$ induced neuronal injuries.

4. Discussion

In the present study, we found that a natural diarylheptanoid AO-2 significantly alleviated neuronal injuries induced by $A\beta_{1\text{-}42}$. $A\beta_{1\text{-}42}$-induced ROS production, apoptosis and necrosis in PC12 cells were all prevented by AO-2. Both cleaved caspase-3 and p-p38 were restored to normal levels after AO-2 treatment, suggesting AO-2 may prevent cell damage and apoptosis by inhibiting caspase-3 and p38 activation by $A\beta_{1\text{-}42}$. In hippocampal neurons, we similarly observed potent protective effects by AO-2, which blocked the damaging effects of $A\beta_{1\text{-}42}$ on neuronal apoptosis and dendrite atrophy. Moreover, we showed that AO-2 prevented the downregulation of PI3K-mTOR pathway induced by $A\beta_{1\text{-}42}$, and the neuroprotective effects of AO-2, including anti-caspase cleavage, antioxidation and dendrite protection, were all dependent on PI3K-mTOR mediated pathways. These findings demonstrate on the cellular levels that AO-2 is a new anti-Aβ compound that may be beneficial for drug development of AD.

Our previous study showed that PI3K-Akt-mTOR pathway is involved in the anti-caspase and dendrite protective effects of AO-1, an analogue of AO-2 [17]. Shown in this study, PI3K-Akt-mTOR is also critical for the protective effects of AO-2. Moreover, p38 inhibition is a newly reported beneficial effect of this diarylheptanoid family in neuronal cells. P38 activation is known to be linked with AD because it can both crosslink with caspase activation to trigger apoptosis and act as a master kinase to cause neuroinflammation [23,24]. As AO-2 potently inhibits p38 phosphorylation, it will be important to delineate whether AO-2 also affects inflammation. Moreover, how AO-2 acts on p38 and PI3K-mTOR pathways awaits further investigation.

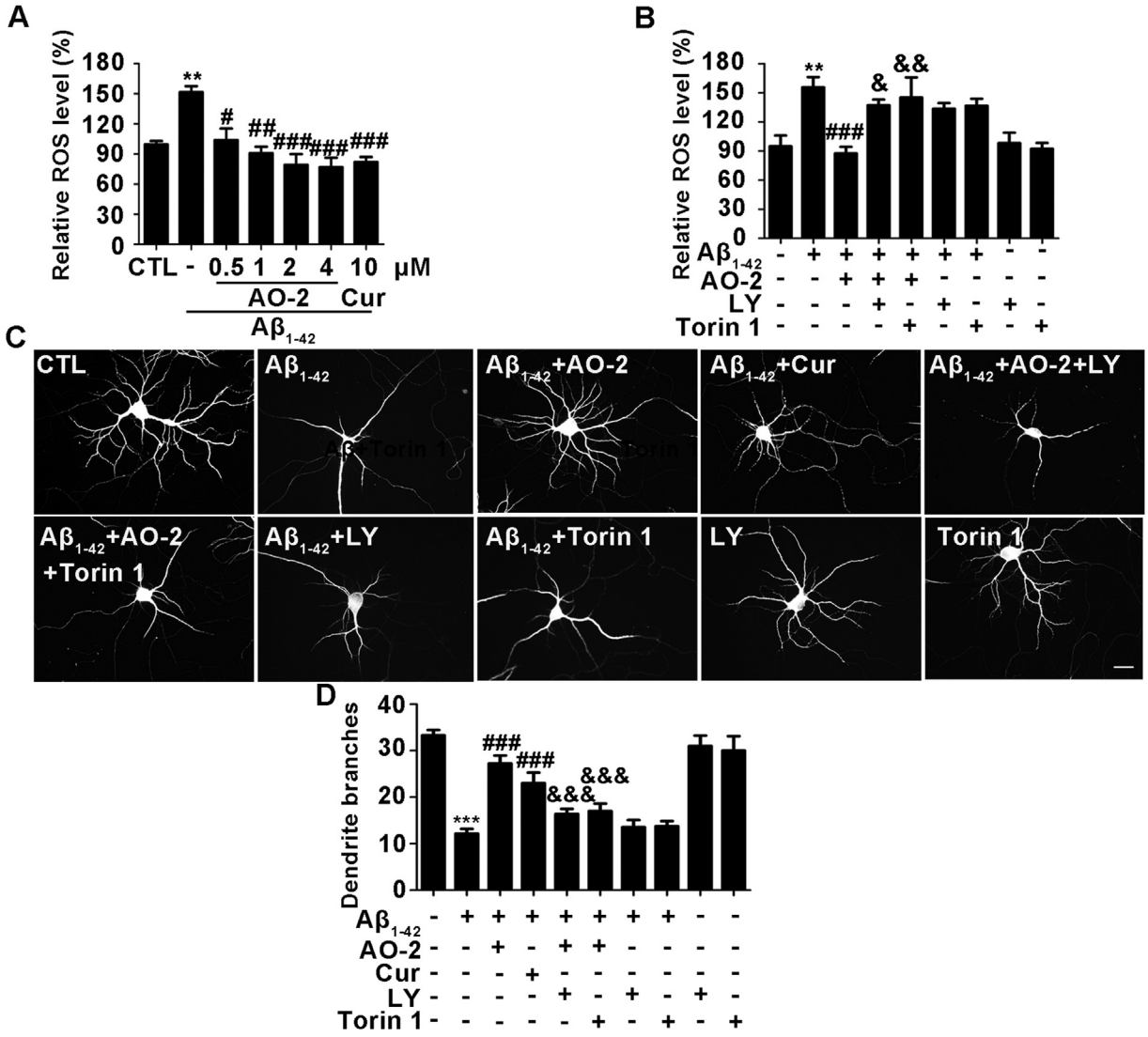

Fig. 4. AO-2 prevents $A\beta_{1-42}$-induced generation of reactive oxygen species (ROS) and dendritic impairments. **A**. Cells were exposed to $A\beta_{1-42}$ (1 μM) or pretreated with various concentrations of AO-2 (0.5, 1, 2 or 4 μM) for 2 h before exposure to $A\beta_{1-42}$ (1 μM) for 24 h. Formation of ROS was assayed by measuring the fluorescence of dichlorofluorescein (DCF). $^{**}P < 0.01$, $A\beta_{1-42}$ vs. CTL; $\#P < 0.05$, $\#\#P < 0.01$ and $\#\#\#P < 0.001$, AO-2 + $A\beta_{1-42}$ or curcumin (Cur) + $A\beta_{1-42}$ vs. $A\beta_{1-42}$ alone. **B**. PC12 cells were pretreated with LY294002 (LY; 10 μM) or Torin-1 (50 nM) for 1 h and exposed to $A\beta_{1-42}$ (1 μM) or pretreated with 4 μM AO-2 for 2 h before exposure to $A\beta_{1-42}$ (1 μM) for 24 h. ROS level was detected by measuring the fluorescence of dichlorofluorescein (DCF). **C**. Hippocampal neurons (DIV 7) were pretreated with LY294002 (LY) or Torin1 for 60 min, followed by AO-2 (4 μM) for 2 h. $A\beta_{1-42}$ (1 μM) peptides were then added for 24 h. One hour prior to AO-2 treatment, LY294002 (LY) and Torin1 were added to cells. Dendrites were shown by MAP2 staining. Scale bar, 20 μm. **D**. Total dendrite branches were counted. $^{**}P < 0.01$ and $^{***}P < 0.001$, $A\beta_{1-42}$ vs CTL; $\#P < 0.05$, $\#\#P < 0.01$ and $\#\#\#P < 0.001$, $A\beta_{1-42}$/Cur + AO-2 vs $A\beta_{1-42}$ alone; $\&P < 0.05$, $\&\&P < 0.01$ and $\&\&\&P < 0.001$, $A\beta_{1-42}$+AO-2+ LY/Torin1 vs $A\beta_{1-42}$+AO-2. 20–30 neurons from three independent experiments in each group were examined. Error bars were mean ± SEM.

Although many pharmacological compounds with anti-oxidative or anti-apoptotic activity are demonstrated to exhibit protective effects against Aβ induced neuronal injury in *in vitro* and *in vivo* studies, natural products represent unique advantages. Curcumin, a natural diarylheptanoid, is a promising compound in the treatment of AD [25,26]. Curcumin significantly reduces Aβ-induced neurotoxicity through the inhibition of oxidative damage [27,28]. Various analogues of curcumin exhibit activities very similar to those of curcumin, however whether they are more effective than curcumin has not been established [29]. AO-2 showed similar effects as curcumin did in both anti-apoptosis and antioxidation, even better effects in p38 inhibition (Fig. 2A and B; Fig. 3A–C; Fig. 4A). Considering that the concentration used for AO-2 (0.5–4 μM) was lower than curcumin (10 μM), it may suggest that AO-2 is a potentially promising compound that is worthwhile for further *in vivo* anti-Aβ studies.

Acknowledgements

We thank Mr. Nan Yao, Mr. Yingjie Li and Ms. Nan Hu for their excellent technical assistance and critical reading of the manuscript. We also thank members of the JNU-HKUST Joint Laboratory for helpful discussions. This work was supported in part by the National Natural Science Foundation of China (Grant nos. 81422012 and 31471046), the Program for New Century Excellent Talents in University of China, and the Special Support (TeZhi) Program of Guangdong Province, China.

Transparency document

Transparency document related to this article can be found online at http://dx.doi.org/10.1016/j.bbrc.2017.01.125.

References

[1] L. Gustafson, A. Brun, J. Risberg, Alzheimer's disease—the most common cause of severe dementia, Lakartidningen 84 (1987) 4139–4143.

[2] L. Liu, W. Wan, W. Chen, Y. Chan, Q. Shen, Y. Li, Yi-Zhi-Fang-dai formula protects against Abeta1-42 oligomer induced cell damage via increasing Hsp70 and Grp78 expression in SH-SY5Y cells, Evid. Based Complement. Altern. Med. 2016 (2016) 8591656.

[3] A. Serrano-Pozo, M.P. Frosch, E. Masliah, B.T. Hyman, Neuropathological alterations in Alzheimer disease, Cold Spring Harb. Perspect. Med. 1 (2011) a006189.

[4] D.J. Selkoe, Amyloid beta-protein and the genetics of Alzheimer's disease, J. Biol. Chem. 271 (1996) 18295–18298.

[5] D.R. Borchelt, G. Thinakaran, C.B. Eckman, M.K. Lee, F. Davenport, T. Ratovitsky, C.M. Prada, G. Kim, S. Seekins, D. Yager, H.H. Slunt, R. Wang, M. Seeger, A.I. Levey, S.E. Gandy, N.G. Copeland, N.A. Jenkins, D.L. Price, S.G. Younkin, S.S. Sisodia, Familial Alzheimer's disease-linked presenilin 1 variants elevate Abeta1-42/1-40 ratio in vitro and in vivo, Neuron 17 (1996) 1005–1013.

[6] P. Mao, P.H. Reddy, Aging and amyloid beta-induced oxidative DNA damage and mitochondrial dysfunction in Alzheimer's disease: implications for early intervention and therapeutics, Biochim. Biophys. Acta 1812 (2011) 1359–1370.

[7] A.M. Szczepanik, D. Rampe, G.E. Ringheim, Amyloid-beta peptide fragments p3 and p4 induce pro-inflammatory cytokine and chemokine production in vitro and in vivo, J. Neurochem. 77 (2001) 304–317.

[8] D.A. Butterfield, C.M. Lauderback, Lipid peroxidation and protein oxidation in Alzheimer's disease brain: potential causes and consequences involving amyloid beta-peptide-associated free radical oxidative stress, Free Radic. Biol. Med. 32 (2002) 1050–1060.

[9] Y. Wang, X.T. Fu, D.W. Li, K. Wang, X.Z. Wang, Y. Li, B.L. Sun, X.Y. Yang, Z.C. Zheng, N.C. Cho, Cyanidin suppresses amyloid beta-induced neurotoxicity by inhibiting reactive oxygen species-mediated DNA damage and apoptosis in PC12 cells, Neural Regen. Res. 11 (2016) 795–800.

[10] J.L. Robinson, L. Molina-Porcel, M.M. Corrada, K. Raible, E.B. Lee, V.M. Lee, C.H. Kawas, J.Q. Trojanowski, Perforant path synaptic loss correlates with cognitive impairment and Alzheimer's disease in the oldest-old, Brain 137 (2014) 2578–2587.

[11] A. Brun, E. Englund, Regional pattern of degeneration in Alzheimer's disease: neuronal loss and histopathological grading, Histopathology 41 (2002) 40–55.

[12] T. Wisniewski, B. Frangione, Immunological and anti-chaperone therapeutic approaches for Alzheimer disease, Brain Pathol. 15 (2005) 72–77.

[13] I. Ferrer, Altered mitochondria, energy metabolism, voltage-dependent anion channel, and lipid rafts converge to exhaust neurons in Alzheimer's disease, J. Bioenerg. Biomembr. 41 (2009) 425–431.

[14] M. Garcia-Alloza, L.A. Borrelli, A. Rozkalne, B.T. Hyman, B.J. Bacskai, Curcumin labels amyloid pathology in vivo, disrupts existing plaques, and partially restores distorted neurites in an Alzheimer mouse model, J. Neurochem. 102 (2007) 1095–1104.

[15] S.D. Rege, T. Geetha, G.D. Griffin, T.L. Broderick, J.R. Babu, Neuroprotective effects of resveratrol in Alzheimer disease pathology, Front. Aging Neurosci. 6 (2014) 218.

[16] G. Tang, X. Dong, X. Huang, X.J. Huang, H. Liu, Y. Wang, W.C. Ye, L. Shi, A natural diarylheptanoid promotes neuronal differentiation via activating ERK and PI3K-Akt dependent pathways, Neuroscience 303 (2015) 389–401.

[17] X. Huang, G. Tang, Y. Liao, X. Zhuang, X. Dong, H. Liu, X.J. Huang, W.C. Ye, Y. Wang, L. Shi, 7-(4-Hydroxyphenyl)-1-phenyl-4E-hepten-3-one, a diarylheptanoid from alpinia officinarum, protects neurons against amyloid-beta induced toxicity, Biol. Pharm. Bull. 39 (2016) 1961–1967.

[18] L. Shi, W.Y. Fu, K.W. Hung, C. Porchetta, C. Hall, A.K. Fu, N.Y. Ip, Alpha2-chimaerin interacts with EphA4 and regulates EphA4-dependent growth cone collapse, Proc. Natl. Acad. Sci. U. S. A. 104 (2007) 16347–16352.

[19] T. Wada, J.M. Penninger, Mitogen-activated protein kinases in apoptosis regulation, Oncogene 23 (2004) 2838–2849.

[20] M.T. Islam, Oxidative stress and mitochondrial dysfunction-linked neurodegenerative disorders, Neurol. Res. (2016) 1–10.

[21] C.D. Fan, Y. Li, X.T. Fu, Q.J. Wu, Y.J. Hou, M.F. Yang, J.Y. Sun, X.Y. Fu, Z.C. Zheng, B.L. Sun, Reversal of beta-amyloid-induced neurotoxicity in PC12 cells by curcumin, the important role of ROS-mediated signaling and ERK pathway, Cell Mol. Neurobiol. (2016), http://dx.doi.org/10.1007/s10571-016-0362-3.

[22] J.J. Palop, L. Mucke, Amyloid-beta-induced neuronal dysfunction in Alzheimer's disease: from synapses toward neural networks, Nat. Neurosci. 13 (2010) 812–818.

[23] M. Bujak, I. Ratkaj, E. Markova-Car, D. Jurisic, A. Horvatic, S. Vucinic, J. Lerga, M. Baus-Loncar, K. Pavelic, S. Kraljevic Pavelic, Inflammatory gene expression upon TGF-beta1-induced p38 activation in primary Dupuytren's disease fibroblasts, Front. Mol. Biosci. 2 (2015) 68.

[24] S.K. NaveenKumar, R.M. Thushara, M.S. Sundaram, M. Hemshekhar, M. Paul, C. Thirunavukkarasu, Basappa, G. Nagaraju, S.C. Raghavan, K.S. Girish, K. Kemparaju, K.S. Rangappa, Unconjugated bilirubin exerts pro-apoptotic effect on platelets via p38-MAPK activation, Sci. Rep. 5 (2015) 15045.

[25] Y. Wang, H. Yin, L. Wang, A. Shuboy, J. Lou, B. Han, X. Zhang, J. Li, Curcumin as a potential treatment for Alzheimer's disease: a study of the effects of curcumin on hippocampal expression of glial fibrillary acidic protein, Am. J. Chin. Med. 41 (2013) 59–70.

[26] J.M. Ringman, S.A. Frautschy, G.M. Cole, D.L. Masterman, J.L. Cummings, A potential role of the curry spice curcumin in Alzheimer's disease, Curr. Alzheimer Res. 2 (2005) 131–136.

[27] S.Y. Park, H.S. Kim, E.K. Cho, B.Y. Kwon, S. Phark, K.W. Hwang, D. Sul, Curcumin protected PC12 cells against beta-amyloid-induced toxicity through the inhibition of oxidative damage and tau hyperphosphorylation, Food Chem. Toxicol. 46 (2008) 2881–2887.

[28] S. Bengmark, Curcumin, an atoxic antioxidant and natural NFkappaB, cyclooxygenase-2, lipooxygenase, and inducible nitric oxide synthase inhibitor: a shield against acute and chronic diseases, JPEN J. Parenter. Enter. Nutr. 30 (2006) 45–51.

[29] S. Shishodia, G. Sethi, B.B. Aggarwal, Curcumin: getting back to the roots, Ann. N. Y. Acad. Sci. 1056 (2005) 206–217.